A non-equilibrium ionization code and its applications

Li Ji, Q. Daniel Wang & John Kwan (*Univ. of Massachusetts, Amherst*)

Abstract

We have developed a non-equilibrium ionization code based on updated atomic data. A version of the code has been optimized so that the calculation can be done efficiently and accurately enough for comparison with X-ray CCD spectra. We also self-consistently include recombination into highly excited levels, which is important in some non-equilibrium cases but has generally been ignored in the past. We show example applications to illustrate the characteristics of the code and its combination with various models of gas dynamics.

1. Introduction

Non-equilibrium ionization is an important phenomenon related to many astrophysical processes, such as rapid heating or cooling, in which gas may be under-ionized or over-ionized. A proper modeling of such a departure from the so-called collisional ionization equilibrium (CIE) is essential to the interpretation of various observations.

We have developed a modern non-equilibrium ionization code to facilitate both high spectral resolution X-ray spectroscopy and low (CCD) resolution global spectral characterization. This code uses the most updated atomic data and can be easily combined with gas dynamics calculation. A version of the code is optimized to allow for efficient spectral computation suitable for comparison with X-ray CCD spectra.

2. Code Characteristics:

- based on *CHIANTI* (V4.2, Young et.al. 2003), atomic data and code are separate
- fine structure energy levels have been regrouped and the collisional excitation rates and A-rates have been recalculated in order to save computational time
- including the atomic process of recombinations into highly excited energy levels
- allowing electron temperature evolution due to Columb interaction with ions
- dealing with dynamics and ionization self-consistently

3. Application 1: Stellar cluster wind scenario

Super stellar clusters (SSCs), identified in a wide range of star-forming galaxies, consist of densely-packed massive stars with typical ages of a few Myr. Within a characteristic radius of a few pc or less, winds from individual stars are expected to collide and merge into a so-called stellar cluster wind. Because of the rapid shock heating in a wind-wind collision and fast adiabatic cooling in the subsequent expansion, the systems will run rapidly into a non-equilibrium state. Diffuse X-ray emission has been detected around stellar clusters (e.g. NGC3603, Arches, and Quintuplet clusters; see the poster by H. Dong & Q. D. Wang). Such emission has been modeled as cluster winds; but existing work does not account for the potential non-CIE effect.

A simple adiabatic stellar cluster wind:

To illustrate the characteristics of the non-equilibrium effect, we first adopt a simple adiabatically expanding cluster wind model: a mass input rate $\dot{M} = 3 \times 10^{-3}\ \mathrm{M_\odot\ yr^{-1}}$ and a wind velocity $v = 1000\ \mathrm{kms^{-1}}$. We assume that the wind is initially in a CIE state with temperature $T_0 = 5 \times 10^6$ K at the center and decreases as $T = T_0(r/r_0)^{-4/3}$, where $r_0 = 0.3$ pc is the initial radius. Fig.1 illustrates the effect of the delayed recombination (the saw-teeth features at high energies).

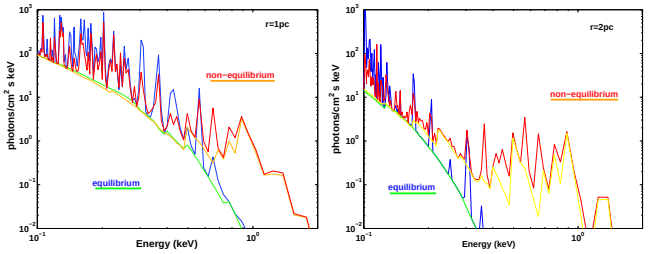

Figure 1. Comparison between the equilibrium (continuum) and non-equilibrium (continuum) calculations of the emission spectra of a stellar cluster wind at radius 1 pc (Left panel) and 2 pc (Right panel).

A more realistic stellar cluster wind model

- assume certain stellar distribution, e.g. exponential law
- steady state and spherical symmetry
- mass and energy inputs proportional to the stellar distribution
- cooling is primarily due to the adiabatic expanding; radiative cooling is negligible
- density and temperature profiles are calculated self-consistently

The surface brightness and the model-predicted spectrum in a given annular region can be calculated and implemented into XSPEC as a table model, taking into account of the projection effect. There are four model parameters:

- mass loss rate $\dot{M}$;
- stellar wind terminal velocity V_∞;
- abundance Z;
- the sonic radius R_s.

Model parameters for the illustration (Fig. 2)

- distance $D = 10\,\mathrm{kpc}$;
- exponential distributed wind profile with sonic radius $R_s = 0.68\ arcmin$;
- $\dot{M} = 1.0 \times 10^{-4}\ \mathrm{M_\odot\ yr^{-1}}$;
- for three values: $V_\infty = 2000, 1000, 500\ \mathrm{km\ s^{-1}}$.

Results are shown in Fig. 3. Spectra are for the two regions: R1=[0, Rs] and R2=[Rs, 2Rs]. The predicted *Chandra* ASIS-S surface brightness are shown for the region [0, 2Rs] and in the two energy bands: B1=[0.3, 2.0] keV, B2=[2.0, 8.0] keV. The solar abundance is assumed.

Non-equilibrium effect is particularly significant for the strong wind (high ratio of total energy to mass inputs). The intensity in the soft energy band could be up to one order of magnitude larger than in the equilibrium case.

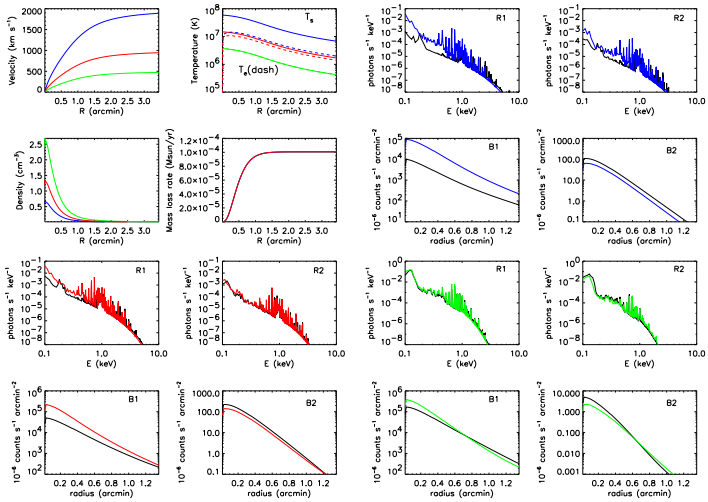

Figure 2. Non-CIE model predictions compared with CIE calculation (black curves). Different colors are for different wind profiles ($V_\infty = 2000,\ 1000,\ 500\ \mathrm{km\,s^{-1}}$)

4. Application 2: Line diagnostics:

As demonstrated in large-scale structure formation simulations, shock-heated warm-hot intergalactic medium (WHIM) represents a main baryons reservoir in the local universe. Observational evidence for the presence of this medium has been revealed from the detection of various UV and X-ray absorption lines (e.g. OVI, OVII, NeVIII). We are currently examining non-CIE effects on the interpretation of these absorption lines. We combine the shock dynamics with our non-CIE code. Fig. 3 compares the ionization fractions of various key ions. Fig. 4 demonstrates the difference between radiative cooling flow prediction and the CIE approximation.

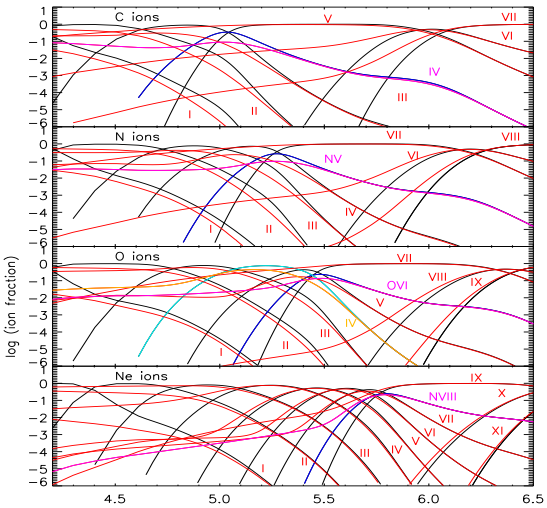

Figure 3. Comparion of the ion fractions for the radiative cooling flow (initially shock-heated to a CIE state with $T_0 = 10^{6.5}$K) between the equilibrium (black, blue and cyan) and non-equilibrium (red, magenta and golden) cases. Solar abundance is assumed.

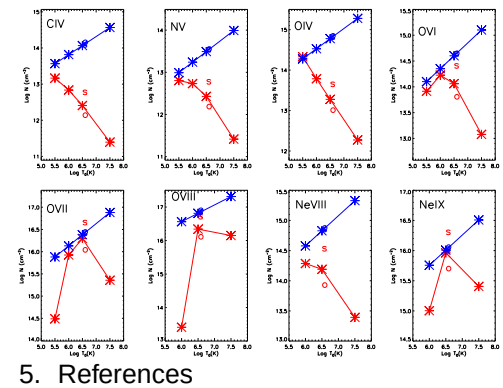

Figure 4: Comparison of radiative cooling column densities between our shock model predictions and the CIE approximation for different shock flows (X axis denotes initial CIE temperature of the shock flow). 'S': $0.5\ \mathrm{Z_\odot}$, 'O': $2.0\ \mathrm{Z_\odot}$, '*' : $1.0 Z_\odot$.

5. References

Savage, B.D., et al. 2005, ApJ, 626, 776
Young, P.R., et al. 2003, ApJS, 144,135